Journal of Electroceramics, 13, 29–33, 2004

Polarization Switching in (100)/(001) Oriented Epitaxial $Pb(Zr,Ti)O_3$ Thin Films

M. TSUKADA,* H. YAMAWAKI, M. KONDO, J.S. CROSS & K. KURIHARA
Fujitsu Laboratories, Ltd., 10-1 Morinosato-Wakamiya, Atsugi, 243-0197, Japan

Submitted February 13, 2003; Revised February 18, 2004; Accepted February 19, 2004

Abstract. Thin films made of (100)/(001)-oriented $Pb(Zr,Ti)O_3$ (PZT) were deposited by liquid-delivery metal-organic chemical vapor deposition on $Ir/MgAl_2O_4/SiO_2/Si(100)$ substrates. For comparison, PZT thin films were also deposited on Ir/MgO(100) substrates. The X-ray Φ scan spectra for the (202) reflections revealed that the PZT films have four-fold symmetry. It indicates that the PZT films were epitaxially grown as a cube-on-cube structure on both substrates. The switchable polarization (Q_{sw}) of the PZT capacitors on the silicon substrate was only 23 $\mu C/cm^2$ at 1.8 V; however, Q_{sw} of PZT capacitors on MgO was 99 $\mu C/cm^2$. In the case of PZT films deposited on silicon, the volume fraction of (001)-oriented domains (which contribute to polarization switching) was 15.1% (calculated from an XRD pattern). This result is due to the lower Q_{sw} of PZT capacitors on silicon. By piezoresponse-force microscopy, switchable and unswitchable domains could be identified by imaging color contrast, namely, (001) and (100) domains, respectively. Consequently, domain distribution of the PZT film on a silicon substrate indicates that the (001) domain exists in the (100) domain matrix.

Keywords: PZT, epitaxial, orientation, polarization, switching, domain, PFM

1. Introduction

Lead zirconate titanate ($Pb(Zr,Ti)O_3$), or PZT, has become the dominant material in ferroelectric random-access-memory (FeRAM) capacitors [1] and in micro electro-mechanical system (MEMS) transducers and actuators [2] because of its higher polarization than other ferroelectrics. In future FeRAM and MEMS applications, even higher switchable polarizations (Q_{sw}) and displacement will be required for ferroelectric capacitors and for piezoelectric transducers and actuators, respectively, as the device-driven dimensions shrink. The polarization properties of PZT thin film capacitors and actuators are related to their film orientation. A titanium-rich tetragonal structure is generally used for PZT materials in piezoelectric and ferroelectric applications because of its high polarization, square shape hysteresis, and high Curie temperature [3]. The polarization direction is aligned with the *c*-axis, (001), in tetragonal PZT. Therefore, if their orientations can be controlled perfectly in (001) direction, the highest Q_{sw} may be obtained. An evaluation of epitaxially grown PZT films is useful in understanding such phenomena.

There have been many experimental studies on depositing epitaxial PZT thin films on single-crystal oxide [4–11] and silicon substrates [12–19]. To develop ferroelectric capacitors, a ferroelectric thin film must be deposited on a conducting material. However, there have not been many studies on epitaxial PZT thin films on conducting materials as a bottom electrode. Also, in device applications, although capacitors must be prepared on silicon, a considerable number of studies have been done on epitaxial PZT thin films on single-crystal oxide substrates, such as MgO and $SrTiO_3$ (STO).

Depending on what references [12–19] are cited, the polarization of epitaxial PZT capacitors on silicon is rather small compared with that of epitaxial PZT capacitors on MgO or STO. To understand this dependence, it is very important to evaluate epitaxial PZT capacitors in same structure on different substrates such as Si and MgO.

*To whom all correspondence should be addressed. E-mail: mtsukada@labs.fujitsu.com

2. Experimental

As substrates, Si(100) and MgO(100) were used. On the Si(100) substrate, a $MgAl_2O_4$ film was deposited by chemical vapor deposition (CVD) and annealed at 1200°C in oxygen and water vapor. As a result, an epitaxial $MgAl_2O_4$ film was formed on the silicon substrate in the form of an $MgAl_2O_4$ (400 nm)/SiO_2(600 nm)/silicon structure. The preparation procedure for $MgAl_2O_4$ on a silicon substrate by CVD is described in detail elsewhere [20]. PZT thin films were deposited on the substrates by liquid-delivery metal-organic chemical-vapor deposition (MOCVD). As for bottom-electrode materials, iridium thin films were formed on MgO(100) and $MgAl_2O_4/SiO_2$/Si(100) films before the PZT deposition. The iridium thin films were deposited at 600°C by RF sputtering to a thickness of 200 nm. As a result, PZT thin films were deposited on the iridium thin films at 560°C by MOCVD with $Pb(thd)_2$, $Zr(OiPr)_3thd$ and $Ti(OiPr)_2(thd)_2$ as precursors and *n*-butyl acetate as the solvent. The thickness of the PZT films was 120 nm.

The composition of the PZT thin films was determined by X-ray fluorescence (XRF), and the crystal structure was evaluated with an X-ray diffractometer (XRD). To measure the electrical properties of the PZT capacitors, 100-nm-thick polycrystalline platinum top electrodes with 500-μm diameter were deposited by sputtering through a metal shadow mask. As for electrical properties, polarization-voltage (P-V) hysteresis and Q_{sw} by PUND method [21, 22] were measured by using a RT6000 ferroelectric tester. The domains of the epitaxial PZT films without top electrodes were evaluated by piezoresponse force microscopy (PFM) [23] with a scanning-probe microscope.

3. Results and Discussion

The B-site composition of the deposited PZT thin films, defined as $Zr/(Zr + Ti)$, was determined by XRF as 0.424, which indicates that the prepared PZT thin films were tetragonal in structure. The XRD $2\theta/\theta$ spectra of the PZT thin films on the silicon and MgO substrates are given in Fig. 1. A strong (100)/(001) peak, but no other peaks, from the PZT appeared and on either the silicon or MgO substrates. The full width at half maximum (FWHM) of the rocking curve of iridium and PZT are 0.80° and 1.23° on MgO, but 0.35° and 1.03° on silicon. PZT on MgO shows better crystallinity; however,

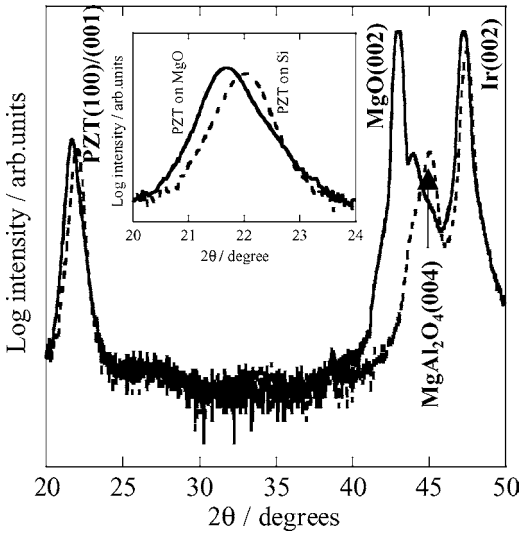

Fig. 1. X-ray diffraction $2\theta/\theta$ scan for PZT/Ir/MgO(100) and PZT/Ir/$MgAl_2O_4/SiO_2$/Si(100). Inset shows enlarged diffraction pattern between 2θ of 20°–24°.

the crystal quality of the PZT thin films is similar on both substrates. According to the X-ray Φ scan spectra of each film on the silicon and MgO substrates, peaks occur 90° apart and nearly at the same azimuth Φ angles as the substrate reflections. This is due to the four-fold symmetry of each film, which is epitaxially grown, i.e., cube-on-cube.

Figure 2 shows the P-V hysteresis loops for the capacitors measured within ±1.8 V on the silicon

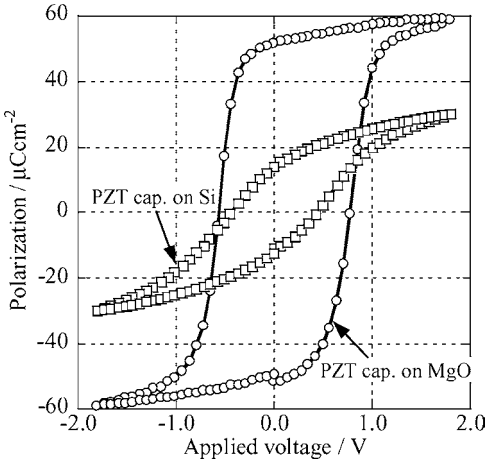

Fig. 2. P-V hysteresis loops of PZT capacitor on both Si and MgO substrates.

and MgO substrates. As mentioned in ref. 10, a PZT capacitor on MgO exhibits a large polarization value and a well squared-shape loop compared with those in the case of silicon. The remanent polarization (Pr) of the PZT capacitor on MgO is 51 μC/cm^2; however, Pr of PZT capacitors on silicon is only 13 μC/cm^2. This is almost one quarter of the value of the PZT capacitor on MgO. The Q_{sw} at 1.8 V was 99 μC/cm^2 for the PZT capacitor on MgO and 23 μC/cm^2 for the PZT capacitor on silicon. The Pr and Q_{sw} value showed the same tendency in both cases. Polarization value of PZT capacitors mainly depend on thickness, composition, crstallinity, and orientation of PZT films. However the thickness and composition of PZT films are same as mentioned above, and the crystallinities of PZT films on MgO and silicon are similar (Fig. 1), the polarization phenomena in both cases are very different. The most likely reason for this difference is the existence of a (100)-oriented domain in the PZT films. In (100)/(001)-oriented PZT capacitors, the magnitude of polarization is determined by the volume fraction of (001) orientation in the films [10]. The inset of Fig. 1 shows enlarged XRD $2\theta/\theta$ spectra of the PZT thin films from 2θ of 20°–24°. The peak split of the (001) and (100) domains is not visible, and the 2θ values of each peak location are not the same. This result indicates a difference in the volume fraction of the (001) and (100) domains. From the $2\theta/\theta$ spectra in the inset of Fig. 1, the (001) and (001) peaks were separated by profile fitting. The volume fraction of the (001) orientation of the PZT films was calculated from a comparison of the integrated area for both peaks [24]. The volume fraction of the (001) orientation of PZT films on MgO and silicon are 84.7% and 15.1%, respectively. As discussed in references [6, 9], if only the misfit of lattice parameters determines the epitaxial relations of a PZT film, both PZT films must have the same volume fraction of the (001) orientation. This is because we used iridium films as bottom electrodes deposited under the same conditions in this study. Therefore, solely the misfit relations of lattice parameters for each film cannot explain the factors determining the volume fraction.

Norga et al. [25] discussed the effect of stress due to the difference in the thermal expansion coefficients (TEC) of stacked film materials during the cooling process from the crystallization temperature of PZT films. The most effective material seems to be the substrate because of its huge volume ratio compared with other film materials. The TECs of silicon and MgO were 3.5×10^{-6}/°C and 10×1010^{-6}/°C, respectively. On the other hand, PZT has a TEC of $6–7\times1010^{-6}$/°C. Compressive stress in the PZT films is caused during cooling due to the small TEC of PZT compared with that of MgO. This makes (001) domains stable on the MgO substrate. However, tensile stress in the PZT films is caused by the larger TEC of PZT than that of silicon. This leads to partial transformation of (001) to (100) domains and lower polarization value of PZT capacitors on silicon.

To understand the domain distribution of the (001) and (100) domains, the PZT films on silicon were observed by PFM. Figure 3 shows a topography and a piezoresponse image of the PZT film on silicon in a 1-μm-square region. The peak-to-valley value is about 10 nm according to Fig. 3(a). The piezoresponse image was obtained in the as-grown state of the PZT films. The initial domain distribution of the PZT film is shown in Fig. 3(b). It is separated into three regions depending

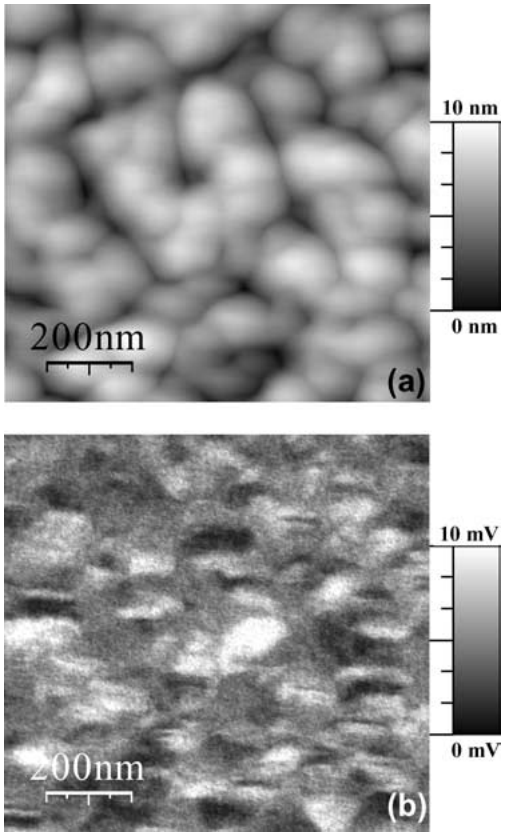

Fig. 3. Topography and piezoresponse image of PZT/Ir/$MgAl_2O_4$/SiO_2/Si: (a) topography and (b) piezoresponse in 1 μm square.

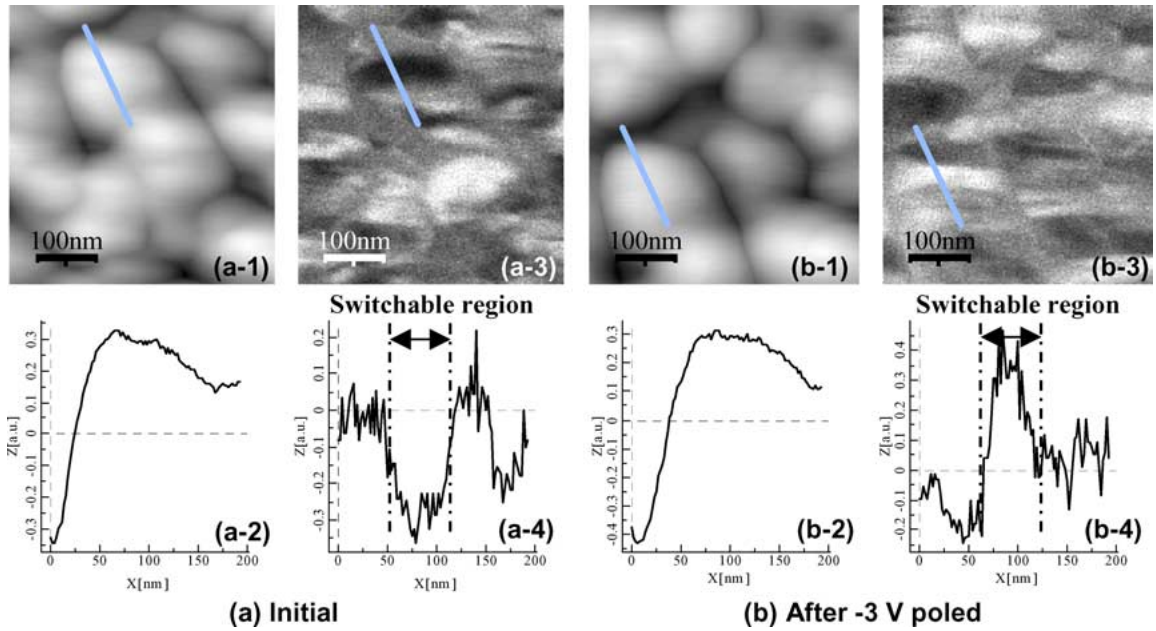

Fig. 4. PFM image of PZT/Ir/$MgAl_2O_4$/SiO_2/Si(100), (a) initial and (b) after −3 V poling. (a-1) and (b-1): topography image; (a-2) and (b-2): topography line profile; (a-3) and (b-3): piezoresponse image; (a-4) and (b-4): piezoresponse line profile. The lines on the images indicate the position of analysis. The line profile analysis were done on same regions as in (a) and (b).

on color contrast, that is, white, black, and gray. To understand the difference in color contrast, the PZT film was poled at −3 V during scanning. Figure 4 shows the topography and piezoresponse results before and after poling. In Fig. 4, (a-2), (a-4), (b-2), and (b-4) indicate the line profiles of topography and piezoresponse, respectively, which correspond with the lines on the above images. The line-profile analysis was done for the same regions in Figs. 4(a) and (b). From Figs. 4(a-2) and (b-2), it is clear that the analyzed regions are the same. That is, the black region in Fig. 4(a-3) corresponds with the valley in Fig. 4(a-4). In the same way, the white region in Fig. 4(b-3) corresponds with the peak in Fig. 4(b-4). And both sides of the black or white regions indicate gray color contrast. From the above results and explanation, it can be interpreted that by poling at −3 V, the black region switched to the white region, but the gray region did not switch by poling. It can thus be said that the black or white region corresponds to the (001) domain, and the gray region correspond to the (100) domain. According to this hypothesis, the piezoresponse image in Fig. 3(b) indicates that the (001) domain such as the black or white region exists in the (100) domain matrix such as the gray region. This interpretation shows qualitatively good agreement with the results of the volume fraction of (001) orientation from the XRD analysis.

4. Conclusions

PZT thin films with iridium bottom electrodes were epitaxially grown on both silicon and MgO substrates. Ferroelectric measurements showed that Q_{sw} of a PZT capacitor on the silicon substrate was about 23 μC/cm^2 at 1.8 V. This is one quarter of that of the PZT capacitors on MgO. This difference in Q_{sw} correlates with the volume fraction of (001) orientation in the PZT films, which seems to be caused by stress that depends on the TEC of the substrate materials. Moreover, PFM analysis showed that the (001) and (100) domains can be distinguished by color contrast.

Acknowledgments

This research was supported by the Grant-in-Aid for the Creation of Innovations through Business-Academic-Public Sector Cooperation (Open Competition for the Development of Innovative Technology) from the

Ministry of Education, Culture, Sports, Science and Technology, Japan.

References

1. G.R. Fox, F. Chu, and T. Davenport, *J. Vac. Sci. Tech. B*, **19**, 1967 (2001).
2. D.L. Polla and L.F. Francis, *Mater. Res. Soc. Bull.*, **21**(7), 59 (1996).
3. G.H. Haertling, *J. Am. Ceram. Soc.*, **82**, 797 (1999).
4. Y.M. Kang, J.K. Ku, and S. Baik, *J. Appl. Phys.*, **78**, 2601 (1995).
5. N. Wakiya, K. Kuroyanagi, Y. Xuan, K. Shinozaki, and N. Mizutani, *Thin Solid Films*, **357**, 166 (1999).
6. K.S. Hwang, T. Manabe, T. Nagahama, I. Yamaguchi, T. Kumagai, and S. Mizuta, *Thin Solid Films*, **347**, 106 (1999).
7. K. Okuwada, K. Yoshida, T. Saitou, and A. Sawabe, *J. Mater. Res.*, **15**, 2667 (2000).
8. A.L. Roytburd, S.P. Alpay, L.A. Bendersky, V. Nagarajan, and R. Ramesh, *J. Appl. Phys.*, **89**, 553 (2001).
9. J. Ishida, T. Yamada, A. Sawabe, K. Okuwada, and K. Saito, *Appl. Phys. Lett.*, **80**, 467 (2002).
10. H. Funakubo, M. Aratani, T. Oikawa, and K. Tokita, and K. Saito, *J. Appl. Phys.*, **92**, 6768 (2002).
11. K. Takahashi, T. Oikawa, K. Saito, H. Fujisawa, M. Shimizu, and H. Funakubo, *Jpn. J. Appl. Phys.*, **41**, 6873 (2002).
12. A.A. Talin, S.M. Smith, S. Voight, J. Finder, K. Eisenbeiser, D. Penunuri, Z. Yu, P. Fejes, T. Eschrich, J. Curless, D. Convey, and A. Hooper, *Appl. Phys. Lett.*, **81**, 1062 (2002).
13. B. Yang, S. Aggarwal, A.M. Dhote, T.K. Song, R. Ramesh, and J.S. Lee, *Appl. Phys. Lett.*, **71**, 356 (1997).
14. S. Horita, A. Horii, and S. Umemoto, *Jpn. J. Appl. Phys.*, **37**, 5141 (1998).
15. S. Horii, S. Yokoyama, T. Kuniya, and S. Horita, Jpn. *J. Appl. Phys.*, **39**, 2114 (2000).
16. A. Sakurai, X.M. Li, K. Shiratsuyu, K. Tanaka, and Y. Sakabe, *Jpn. J. Appl. Phys.*, **39**, 5441 (2000).
17. S. Horita, T. Toda, and H. Kasagawa, *Jpn. J. Appl. Phys.*, **41**, 6653 (2002).
18. Y. Wang, C. Ganpule, B.T. Liu, H. Li, K. Mori, B. Hill, M. Wuttig, R. Ramesh, J. Finder, Z. Yu, R. Droopad, and K. Eisenbeiser, *Appl. Phys. Lett.*, **80**, 97 (2002).
19. W.M. Gilmore III, S. Chattopadhyay, A. Kvit, A.K. Sharma, C.B. Lee, W.J. Collis, J. Sankar, and J. Narayan, *J. Mater. Res.*, **18**, 111 (2003).
20. M. Ihara, Y. Arimoto, M. Jifuku, T. Kimura, S. Kodama, H. Yamawaki, and T. Yamaoka, *J. Electrochem. Soc.*, **129**, 2569 (1982).
21. S.D. Traynor, T.D. Hadnagy, and L. Kammerdiner, *Integrated Ferroelectrics*, **16**, 63 (1997).
22. T.D. Hadnagy, S.D. Traynor, and D.I. Dalton, *Integrated Ferroelectrics*, **16**, 219 (1997).
23. A. Gruverman, H. Tokumoto, A.S. Prakash, S. Aggarwal, B. Yang, M. Wuttig, R. Ramesh, O. Auciello, and T. Venkatesan, *Appl. Phys. Lett.*, **71**, 3492 (1997).
24. M. Tsukada, M. Mushiga, J. Watanabe, and J.S. Cross, *Jpn. J. Appl. Phys.*, **41**, L1312 (2002).
25. G.J. Norga, S. Jin, L. Fe, D.J. Wouters, H. Bender, and H.E. Maes, *J. Mater. Res.*, **16**, 828 (2001).